PAPER

Compressive yield stress of depletion gels from stationary centrifugation profiles

IOP Publishing Journal of Physics: Condensed Matter
J. Phys.: Condens. Matter **30** (2018) 044005 (7pp) https://doi.org/10.1088/1361-648X/aaa2d1

Compressive yield stress of depletion gels from stationary centrifugation profiles

Enrico Lattuada, Stefano Buzzaccaro and Roberto Piazza

Department of Chemistry, Materials Science, and Chemical Engineering (CMIC), Politecnico di Milano, Edificio 6, Piazza Leonardo da Vinci 32, 20133 Milano, Italy

E-mail: enrico.lattuada@polimi.it

Received 5 October 2017, revised 15 December 2017
Accepted for publication 19 December 2017
Published 4 January 2018

Abstract

We have investigated the stationary sedimentation profiles of colloidal gels obtained by an arrested phase-separation process driven by depletion forces, which have been compressed either by natural gravity or by a centrifugal acceleration ranging between $6g$ and $2300g$. Our measurements show that the gel rheological properties display a drastic change when the gel particle volume fraction exceeds a value ϕ_c, which barely depends on the strength of the interparticle attractive forces that consolidate the network. In particular, the gel compressive yield stress $\Pi(\phi)$, which increases as $\Pi(\phi) \sim \phi^{4.2}$ for $\phi \lesssim \phi_c$, displays a diverging behaviour for $\phi > \phi_c$, with an asymptotic value that is close to the random close packing value for hard spheres. The evidence we obtained suggests that ϕ_c basically coincides with the liquid (colloid-rich) branch of the metastable coexistence curve, rather than with the lower (and ϕ-dependent) values expected for an attractive glass line penetrating inside the coexistence region.

Keywords: disperse systems, gels, depletion forces, glasses, analytical centrifugation, compressive rheology

(Some figures may appear in colour only in the online journal)

1. Introduction

The phase diagram of systems of colloidal particles interacting via a short-ranged attractive potential, due for instance to depletion forces, displays a coexistence gap, which, although metastable with respect to crystallization, is the analogous of the gas–liquid (G–L) transition for a pure fluid [1]. Hence, when the colloid is quenched inside this gap by increasing the strength of the attractive forces, the system starts undergoing a phase separation into a colloid rich and a colloid poor phase. Except for very shallow quenches, however, the phase separation process does not reach completion, and the system gets arrested into a disordered gel phase. Arrested phase separation is in fact the main route to gelation for isotropic interaction potentials [2, 3]. Since the line bounding the phase-separation region is very flat, the binodal and spinodal lines are pretty close, thereby phase separation proceeds very similarly to a spinodal decomposition process even if the particle volume fraction is consistently lower than its critical point value. Consequently, while undergoing phase separation, the system displays a characteristic length scale, corresponding to the typical size of the clusters that progressively grows up to a maximum value that is smaller the deeper the quench into the coexistence gap [4]. Confocal microscope observations [5] show that, when the initial particle concentration is even moderately large (a few percent), these clusters are much more compact than those obtained in the irreversible aggregation of very diluted colloidal suspensions. Therefore, gels forming by arrested phase separations are intrinsically made of rather compact clusters, linked by relatively weak intercluster bonds. Unless the particle density is closely matched with that of the solvent, these gels usually collapse or compress under the effect of the gravitational stress depending on the initial particle concentration and on the quench depth, so that the clusters progressively consolidate and eventually merge, at least partially, generating a less heterogeneous network [6–8].

However, which is the typical value ϕ_c of the particle volume fraction in the clusters that initially form during the phase separation process? A first and rather reasonable guess is that ϕ_c coincides with the volume fraction of

the *equilibrium* dense phase, namely with the liquid branch of G–L coexistence curve. Yet, since the two phases are not macroscopically separated, evaluating ϕ_c is far from being trivial. In fact, splitting the system volume between the two phases requires substituting the diffuse interface between them, whose thickness is of the order of the system correlation length (basically coinciding with the particle size, unless the quench is extremely shallow), with a Gibbs' dividing line. Nevertheless, two distinct statistical methods used to analyze the cluster images obtained by confocal microscopy suggest that $\phi_c \simeq 0.55-0.60$ and that this value weakly depend on the interaction strength and on the initial particle concentration [5, 9], although it is worth noticing the clusters measured in [9] seems to slowly compact with gel ageing. A more refined statistical analysis of depletion gels obtained in numerical simulations [10] (but which could in principle be used for analyzing confocal images of real gels) actually suggests that, although the average value of ϕ_c is comparable to those found in [5, 9], the clusters are rather inhomogeneous, with a radial density profile that increases towards the center of the cluster up to values that are of the order of the random close packing of spheres $\phi_{\rm rcp} \simeq 0.64$.

The experimental results we referred to were obtained for suspensions of large (in the hundred of nanometers size rage) spherical particles, in which gelation is driven by the depletion forces induced by a macromolecular additive. Apparently, the scenery seems to be quite different for aqueous solutions of small globular proteins, in which gelation, although still taking place via an arrested G–L phase separation, is presumably driven by the attractive forces associated with the presence of hydrophobic patches on the particle surface. In fact, a combined ultra-small angle light scattering and video microscopy investigation of lysozyme gels [11] suggests that the dense protein phase has a volume fraction which is much lower than the values found in [5, 9] and that consistently decreases with increasing strength of the attractive potential, reaching values as low as $\phi_c \simeq 0.2$ for deep quenches within the G–L coexistence gap. On the basis of this evidence, the authors conclude that, unless the quench inside the metastable gap is very shallow, the volume fraction of the dense phase that forms is rather fixed by an attractive glass line inside the G–L coexistence, so that dynamic arrest takes place much before the equilibrium high-density phase is reached. That the volume fraction of the arrested phase cannot be higher that the values obtained in [11] seems to be supported by the fact that the gels cannot be further compressed even if subjected to a centrifugal force as large as 2.3×10^4 g [12]. Comparing their results with those obtained for colloidal depletion gels in [5], the authors admit that the patchy and rather asymmetric nature of the attractive potential in lysozyme solutions may have some effects on the gelation process, but mostly attribute the inconsistency between the two sets of results to the ambiguity of the method used to evaluate ϕ_c in [5].

As we already mentioned, subsequent experimental and numerical results seems to suggest that the conclusions reached in [5] basically hold regardless of the specific method used to evaluate ϕ_c. Nevertheless, it is hard to state that conclusions solely reached by a statistical analysis of real-space cluster images do not possess some degree of arbitrariness. The purpose of this paper is showing that valuable and unambiguous information can be obtained by investigating the *mechanical* properties of colloidal gels derived from natural and forced sedimentation measurements, which already proved to be a powerful method to obtain not only the equilibrium equation of state of a colloidal system, but also the rheological properties of nonequilibrium arrested phases [13]. In particular, we plan to show that the particle volume fraction dependence of the yield stress of depletion gels drastically changes from a power law behavior to an extremely fast increase around a volume fraction ϕ_c that barely depends on the strength of the attractive interaction, and which is pretty close to the values found in [5, 9]. This evidence, derived from macroscopic rheological measurement, strongly support the suggestion that the dense phase forming in the spinodal decomposition process is pretty close to the liquid branch of the binodal line.

2. Experimental

2.1. Colloidal system

The system we used consists of monodisperse spherical particles with a radius $R = 90 \pm 3$ nm made of MFA, a polytetrafluoroethylene copolymer. Since this material is partially crystalline, the light scattered by MFA particles has a depolarized component that is not influenced by interparticle interactions (namely, it is a purely incoherent contribution to the scattered light) and is strictly proportional to the local particle concentration. This depolarized scattered component can easily be set apart by matching the refractive index n_s of the solvent to the average particle refractive index $\bar{n}_p = 1.355$, so to remove the stronger polarized scattering contribution [14]. In these index-matching conditions, the intensity of the scattered light becomes an accurate probe of inhomogeneous concentration profiles like those generated by gravity settling. A further advantage of these particles is that the density of MFA ($\rho = 2.14$ g ml^{-1}) is much higher than the density of water, which allows a much more precise determination of the particle volume fraction to be made compared to the case of other common colloidal systems like polystyrene or PMMA particle suspensions.

The particles are suspended in solutions of Triton X100, a nonionic surfactant that forms globular micelles with a radius $a \simeq 3.5$ nm, acting as a depletant for the MFA particles. Former measurements of equilibrium sedimentation profiles have provided a full characterization of this system in terms of equation of state and phase diagram, yielding a detailed quantitative mapping of the suspension onto a model system of adhesive hard spheres (AHS, [2]). Besides, a surfactant monolayer also adsorbs on the particle surface, acting as a steric stabilization layer that allows one increasing the suspension ionic strength so to screen electrostatic interactions. To ensure full screening, all investigated samples were prepared in the presence of 250 mM NaCl, corresponding to a Debye–Hückel length of about 0.6 nm, which is consistently smaller than the thickness of the stabilizing surfactant layer. Refractive index

measurements give $n_s = 1.3355 + 1.467 \times 10^{-4} c_s$, where c_s is the Triton concentration in g l^{-1}. Hence, the index matching condition is met for $c_s \simeq 132$ g l^{-1} (about 12.4% in surfactant volume fraction), which indeed yields a minimum in the scattering intensity.

2.2. Analytical centrifugation

Measurements of the sedimentation profiles were performed using an analytical centrifuge (LUMiSizer, Lum GmbH), which allows to monitor simultaneously the settling profile of up to 12 samples by measuring their optical extinction profile with a linear detector array with an accurate temperature control in the range 4 °C $\leqslant T \leqslant$ 40 °C. For a concentrated dispersion, this usually yields just a semi-quantitative concentration profile, because the sample transmittance depends not only on concentration, but also on the structure factor of the suspension. As formerly discussed, however, for MFA suspensions in index-matching condition, the natural extinction measured by the centrifuge sensor turns out to be strictly proportional to the local particle volume fraction ϕ. In what follows, we shall quantify the strength of the artificial gravity in the centrifuge using the so-called relative centrifugal force $\mathrm{RCF} = \omega^2 r/g$, where ω is the angular velocity of the rotor, r the distance from the center of rotation, and g the gravity acceleration. At variance with experiments in natural gravity, this force obviously depends on position. For the centrifuge we used, however, the centrifugal force changes by only 7×10^{-3} mm^{-1}. Since the sedimentation profiles we measured extend by no more than 15 mm, this only amounts to an overall change of about 10% over the whole profile. Nevertheless, this small effects was fully taken into account while investigating the stationary sedimentation profiles (see section 3.2). For the sake of convenience, however, the RCF values given for the profiles discussed in the text are calculated for $r = R$, where R is the distance of the cell bottom from the center of rotation.

Measurements were made at variable centrifugal forces, ranging between 6 RCF and 2300 RCF. In addition, we also performed measurements in natural gravity conditions. In detail, the experimental protocol we adopted for all investigated samples is the following:

(i) The sample is poured in an optical cuvette suitable for centrifugation and left settle outside the centrifuge for 30 d to reach mechanical equilibrium in natural gravity.
(ii) The cuvette is then gently inserted in the centrifuge and spun at the lowest value of RCF, and time evolution of the settling profile is periodically measured, until it reaches a stationary condition when no further changes of can be detected (for measurements performed at RCF = 6, this typically requires several days). At this stage, a detailed measurement of the profile is taken.
(iii) The centrifugal speed is then increased to the next selected value of RCF, and the further compression of the *same* sample is monitored until it reaches a new stationary profile, which is again measured before moving to the next value of RCF, repeating the same operations in pre-selected steps until the maximal centrifugal speed (RCF $\simeq$ 2300) is reached.

To inquire about the possible occurrence of history-depending effects, we also prepared several samples at the same initial particle volume fraction ϕ_0 and depletant concentration c_s, separately centrifuging directly (namely, not in progressive steps) at each one of the selected RCF values. The stationary profiles obtained using this alternative method did not show any appreciable difference from those obtained by subjecting the samples to the previously described stepwise increase of the RCF.

2.3. Yield stress determination by compressive rheology

The distinctive property of all soft materials is that they weakly resist to *shear* stress, while for what concerns *volume* changes, they are basically incompressible like a simple fluid or solid. This does not mean, however, that the *dispersed phase* cannot be squeezed to a smaller volume by expelling part of the solvent. This can be done either by selective filtration, by using special 'vane rheometers' [15, 16], or, more simply, by subjecting the dispersed phase and the solvent to different forces, which is what naturally happens in a centrifuge when the two phases have a different density. Natural or forced sedimentation can therefore be exploited to perform *compressive rheology*, a relatively recent term used to generically indicate these 'squeezing' techniques, which find applications in several fields (for a comprehensive review, see [17]). Very often, when the investigated material is a colloidal gel, the squeezing process is irreversible even for quite small values of the compressive stress, namely the network undergoes a plastic deformation. A widely used theoretical analysis of the plastic squeezing of a disordered colloidal solid is due to Buscall and White [18]. In this approach, modeling the kinetics of the plastic consolidation process requires as input both the mechanical strength of the network, quantified by compressive yield stress $\Pi(\phi)$, and the rate of escape of the solvent, which is in turn fixed by the permeability of the network. The latter quantity, which is usually quite hard to figure out, is not required, however, to evaluate the final stationary state of the network. The physical motivation for using $\Pi(\phi)$ to quantify the strength of the latter is that a portion of the gel at local solid volume fraction ϕ does not undergo any deformations until the applied stress on the network exceeds the compressive yield stress $\Pi(\phi)$. When this happens, the structure collapses, structural consolidation occurs, and the local volume fraction increases. This compaction process goes on until, all over the sample, the local volume fraction reaches a value that is large enough so that $\Pi(\phi)$ is barely sufficient to sustain the compressive stress due to the (natural or, in a centrifuge, effective) weight of the material lying above. In the case of a centrifugal field, balancing the forces on a volume element yields an expression for $\Pi(\phi)$ which is a simple generalization to a position-dependent centrifugal force of the expression for the osmotic pressure associated with the equilibrium sedimentation profiles in natural gravity [13],

$$\Pi(z) = \omega^2 \Delta\rho \int_{R-z}^{R-h} x\phi(x)\,\mathrm{d}x, \qquad (1)$$

where $\Delta\rho$ is the density difference between the solid and the solvent, h is the final height of the gel, and z is the distance from the cell bottom. Hence, finding the full dependence of the yield stress on ϕ only requires a numerical integration of the volume fraction profile, provided of course that the local concentration profile can be quantitatively measured, which, as we shall see, is the case of the index-matched suspensions discussed in section 3.2.

3. Results

3.1. Phase diagram

The experimental phase diagram of the investigated system displayed in figure 1 shows the binodal and spinodal lines bounding from below the coexistence gap. The spinodal line was determined by progressively increasing the concentration of Triton X100 in very small steps ($\leqslant 1$ g l^{-1}), letting the sample equilibrate for several minutes, and monitoring the intensity of a laser beam transmitted through the sample. The spinodal line is assumed to be reached when the sample transmittance drops to zero, which generally occurs for a well defined value of c_s. Once this condition was reached, the samples were quenched inside the coexistence gap by further addition of a variable amount of surfactant, which led to phase separation. When the meniscus separating the two phases had reached a steady position within the sample, which typically occurs in a couple of hours, the composition of the two coexisting phases was obtained by measuring the ratio of their volumes, sampling the upper dilute phase, and measuring its density with a Anton Paar DMA35 oscillating capillary densimeter.

Figure 1 shows that the nature and volume fraction of the lower phase resulting from the phase separation process strongly depends on the quench depth. For $c_s \lesssim 80$ g l^{-1}, which is only about 5% larger that the minimum amount of surfactant needed to induce phase separation, the suspension separates into two fluid phases, whose compositions indicates the gas and liquid branches of the binodal coexistence line (in passing, note that the latter basically coincides with the spinodal line). However, for $c_s \gtrsim 84$ g l^{-1}, the lower phase is actually a gel displaying a finite yield modulus, and a particle volume fraction which rapidly decreases with increasing c_s. For these samples, measurements of the composition of the two phases were taken just at the end of the first relatively fast descent of the meniscus, before the much slower gel compression stage starts [6]. The observed gel-like phase may then be regarded as composed of weakly-bonded clusters that rapidly settle because the tenuous network that forms during the phase separation process cannot sustain the gravitational stress, namely these gels belong to the class of 'collapsing' depletion gels [8]. Notice that, although the line joining the observed gel phases looks qualitatively similar to a kind of prolongation within the coexistence gap of the attractive glass line experimentally observed for depleted colloids at higher concentration, glasses are not expected to display the characteristic structural length scale (the cluster size) occurring in gels obtained by arrested spinodal decomposition.

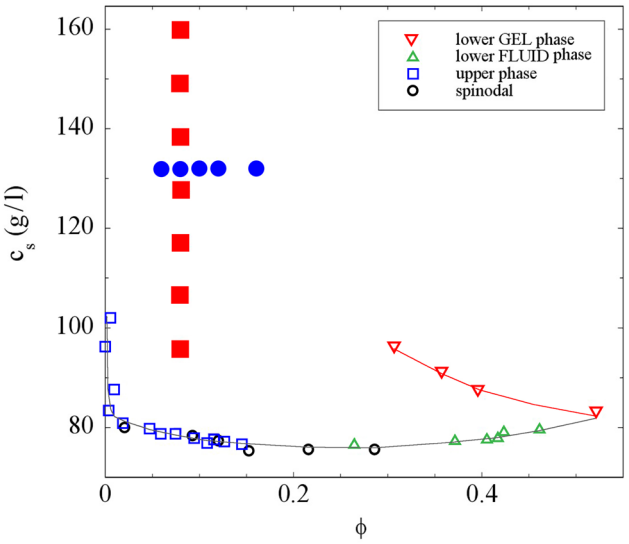

Figure 1. Phase behavior of suspensions of MFA particles suspended in water + 250 mM NaCl, in the presence of a concentration c_s of added surfactant. The full dots show the composition of the samples investigated at constant surfactant concentration, corresponding to the index-matching condition $c_s \simeq 132$ g l^{-1}, while the full squares indicates the samples investigated by varying the surfactant concentration, and therefore the strength of attractive interactions, at constant initial particle volume fraction $\phi_0 = 0.08$.

Figure 1 also shows the composition of the samples investigated in the next sections. The full dots correspond to the series of samples prepared at constant surfactant concentration $c_s = 132$ g l^{-1} that, as already mentioned, corresponds to the index-matching condition. This allowed us to accurately determine the gel sedimentation profiles under variable centrifugal force using the method described in section 2.3. Conversely, the series of samples at constant initial particle volume fraction ϕ_0 (full dots in the figure) is not in perfect index-matching conditions, which prevents from obtaining accurate and quantitative volume fraction profiles. Nevertheless, in section 3.3 we show that even an approximate evaluation of the average particle fraction in the sediment still provides very useful information on the dependence of ϕ_c on the interaction strength.

3.2. Compressive yield stress of depletion gels at fixed interaction strength

We first discuss the results obtained for gels at different initial particle volume fraction ϕ_0, where the strength of the depletion interactions is fixed by the amount of depletant. The inset of figure 2 shows two representative equilibrium profiles for gels at $\phi_0 = 0.08$ compressed at two different values of RCF. For the lowest accessible value of RCF $= 6$, the volume fraction profile smoothly grows from $\phi = 0$ to $\phi \simeq 0.56$, although for $\phi \simeq 0.33$ a change of slope can be noticed. It is hard to unambiguously state whether the region with $\phi \lesssim 0.33$ truly

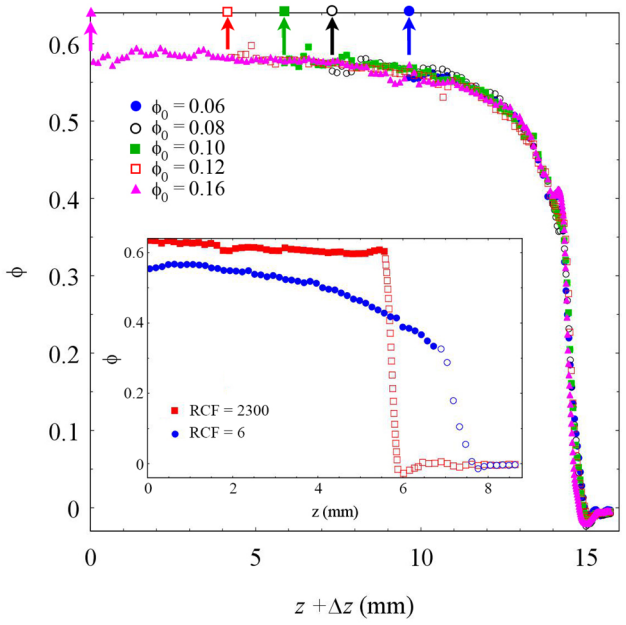

Figure 2. Inset: equilibrium profiles for MFA depletion gels at fixed initial particle volume fraction $\phi_0 = 0.08$ and depletant concentration $c_s = 132\,\mathrm{g\,l^{-1}}$, obtained at relative centrifugal force RCF = 6 (circles) and RCF = 2300 (squares). Data considered for evaluating the gel yield stress are shown by full symbols. Body: Scaling of the volume fraction profiles at RCF = 10, obtained by translating the profiles along the z-axis of an amount Δz with respect to the profile obtained at $\phi_0 = 0.16$. For each curve Δz can be obtained from the position of the cell bottom, indicated by the arrows and the corresponding symbols at the top of the plot (for instance, $\Delta z = 5.8$ mm for $\phi_0 = 0.10$).

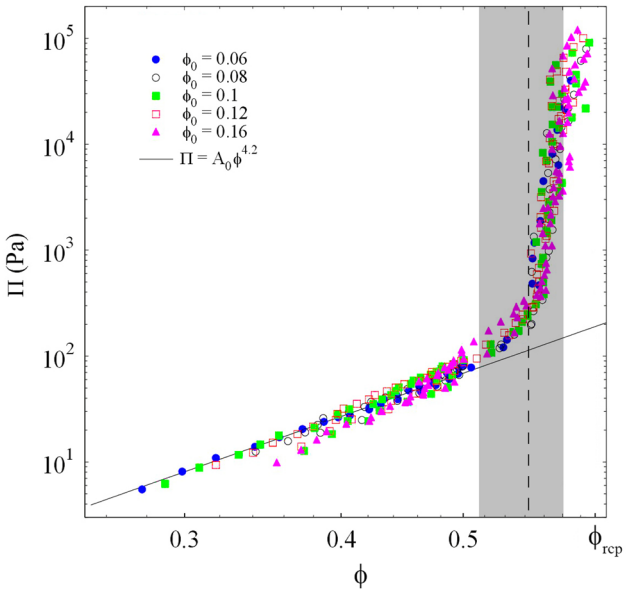

Figure 3. Compressive yield stress as a function of ϕ at fixed depletant concentration $c_s = 132\,\mathrm{g\,l^{-1}}$, corresponding to the index-matching condition, and different values of ϕ_0. Each curve is obtained by joining the results calculated, using equation (1), from the profiles obtained at 7 different values of RCF ranging from RCF = 6 to RCF = 2300. The full line is a power-law fit $\Pi = A_0\phi^{\alpha}$ to the data with $\phi < 0.5$, giving an exponent $\alpha = 4.2$ and an amplitude $A_0 = 1265$ Pa. The whole range ($0.52 \lesssim \phi \lesssim 0.60$) spanned by values for the liquid branch obtained by Lu *et al* ([5], figure 4(d)) and Bartlett *et al* ([9], figure 1) is indicated by the grey-shaded rectangle, and its average value $\phi \simeq 0.565$ by the dashed line. $\phi_{rcp} \simeq 0.64$ is the random close packing value for hard spheres.

corresponds to an arrested gel, or rather to a still non-equilibrated sediment of non compacted settled clusters. Therefore, we conservatively decided to consider, to evaluate the compressive yield stress according to equation (1), only the sediment region with $\phi \geqslant 0.33$ (full dots). Conversely, the profile obtained for RCF = 2300, is almost a step function, rapidly rising from $\phi = 0$ to an almost constant value $\phi \simeq 0.60$. Similarly as the results obtained in [7] for MFA depletion gels studied in natural gravity, we found that, for a given value of RCF, the shape of the profiles does not depend on the initial particle volume fraction ϕ_0. This is explicitly shown in the body of figure 2 for the profiles obtained at RCF = 10, which nicely superimpose when shifted along the z axis, implying that gels prepared at different ϕ_0 have the same compressive yield stress. A similar rescaling works for all the other investigated values of RCF.

The log–log plot in figure 3, which displays the full dependence of the compressive yield stress Π as a function of the local volume fraction ϕ obtained from the stationary profiles according to equation (1), shows that data for different values of ϕ_0 collapse onto a single master curve. Note that each curve is obtained by joining (without any adjustment) the results for the profiles obtained at several values of RCF. For $\phi \lesssim 0.5$, the yield stress is found to grow as $\Pi = A_0\phi^{\alpha}$, a power-law behavior reported for several colloidal gels, with an exponent $\alpha \simeq 4.2$ that agrees with the value obtained in previous studies of similar depletion gels, at least for $\phi \lesssim 0.4{-}0.45$ [7]. Using a centrifuge allowed us to show that, provided that the compressive stress is high enough, consistently higher values of the sediment volume fraction, approaching the r.c.p. value, can actually be reached. However, the behaviour of $\Pi(\phi)$ drastically changes, starting around $\phi \gtrsim 0.50$, from the aforementioned power-law behaviour to a much more rapidly increasing trend, which apparently diverges for a volume fraction that is of the order of ϕ_{rcp}. Note that, since the compressibility of a random packing of spheres *must* vanish at ϕ_{rcp}, deviation from the power-law behavior should in fact be expected. Such a deviation actually occurs for values of ϕ which are pretty close to the concentration of the cluster phase ϕ_c reported in [5, 9], whose range of values is indicated by the grey-shaded area in figure 3.

3.3. Dependence of the compressive yield stress on the interaction strength

For $c_s \neq 132$ g $\mathrm{l^{-1}}$, the index-matching condition is not exactly met, hence the light scattered from the gels contains a coherent component that does not make the scattered intensity strictly proportional to the local volume fraction. In principle, gels with $c_s < 132$ could be matched by the addition of urea, glycerol, or another high refractive index additive. Yet, this would slightly modify the phase diagram. Besides, there is of course no way of matching the gels made for $c_s > 132$, which turn out to be particularly interesting to investigate the behaviour at high attractive interaction strength. In the past, several methods have been developed to obtain $\Pi(\phi)$ without resorting

to an explicit measurement of the concentration profile. These methods, which just require to measure the stationary sediment height h, are found to be in reasonable agreement with the results of compressive yield stress measurements obtained by macroscopic rheological measurements [17]. However, since they actually require to evaluate the *derivative* of h with respect to the centrifugal force, and therefore to investigate a large number of profiles obtained at different values of RCF, they are very time-consuming. In this work, we shall rather use an approximate but easier approach, which is anyway expected to yield reasonably good data when the profiles show an almost step-like shape (see the inset of figure 2), at least for what concerns the volume fraction dependence of Π on ϕ. From the profile, we can then reasonably estimate the height h of the sediment, which yields an average volume fraction $\bar{\phi} = (h_0/h)\phi_0$, where h_0 is the initial height of the suspension. Our simplifying assumption, which exactly holds for a perfectly uniform, step-like profile, is taking $\phi(z) = \bar{\phi}$ *all over* the profile. Furthermore, since the centrifugal force varies linearly with the distance from the center of rotation, we assume that the whole profile is subjected to a RCF value which is the mean between the extreme values at the top and bottom of the sediment (recall, anyway, that these values differ by a few percent). Hence, for each investigated value of RCF, to the compressive yield stress we attributed the constant value

$$\Pi = \Delta\rho h_0 \phi_0 \omega^2 \left(R - \frac{h}{2}\right). \qquad (2)$$

A first minor problem in using this method is that, when the sediment and the supernatant differ in refractive index, the optical mismatch makes it difficult to give a precise assessment of the position of the interface. In practice, this leads to an uncertainty of about 5% in the estimation of h, and then of $\bar{\phi}$. A subtler and more serious source of inaccuracy is the following. For $z < h$, the stationary profile $\phi(z)$ *cannot* be exactly constant, for this would imply a fully incompressible structure, which is possible only for $\phi \simeq \phi_{\rm rcp}$. It is easy to show that, even assuming a weak linear change of $\phi(z)$ with z, this leads to a consistent error in the estimated value of Π. Besides, for low values of RCF, at which the profile is much smoother, the discrepancy can be quite larger than that. For instance, for the profiles shown in the inset of figure 2 this yields an overestimate of Π of a factor of about 2.5 for the profile obtained at RCF $= 2300$, and of about 5 for the profile at RCF $= 6$. However, it is important to notice that this mostly affects the absolute values of Π, and much less the dependence of Π on ϕ. As a matter of fact, the results for depletion gels subjected to natural gravity in [7] suggest that, at least in the low ϕ-range, the yield stress follows a power-law dependence on ϕ for all investigated values of the depletant concentration, with an exponent that does not depend on c_s, although with a variable amplitude. Hence, even if may expect that the absolute values of the yield stress are affected by a noticeable error, it is anyway worth taking a look at the results for $\Pi(\phi)$ obtained by varying the strength of the depletion forces, tuning them with the amount c_s of depletant.

We then performed experiments for 7 different values of c_s, ranging between 96 and 160 g l^{-1}, both in natural gravity and for either moderate (RCF $= 6, 7, 10$) or large (RCF $= 100, 300, 1000, 2300$) values of the centrifugal acceleration, which for the data presented in figure 2 were respectively associated to the power-law and to the diverging behavior of $\Pi(\phi)$. Figure 4 shows that, when fitted to the low-ϕ behavior $\Pi(\phi) = A\phi^{4.2}$ obtained for the profiles in index-matching conditions, all the experimental curves can approximately be rescaled on a single master curve by dividing $\Pi(\phi)$ by the amplitude value A. Actually, such a rescaling holds for $\phi > 0.5$ too, where the data consistently deviate from a power-law behaviour, suggesting that ϕ_c is barely depending on the depletant concentration c_s. Besides, the fitted values of A, shown in the inset, grow linearly with c_s, in agreement with previous results obtained for other kinds of depletion gels [19].

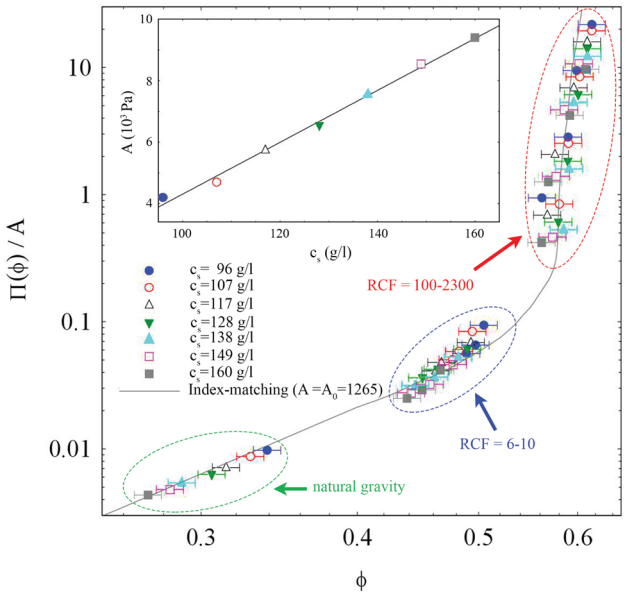

Figure 4. Body: compressive yield stress $\Pi(\phi)$ for several values of c_s, rescaled to the amplitude values A discussed in the text. The full line is obtained as the average of the values obtained in index matching ($c_s = 132$ g l^{-1}) shown in figure 2, also scaled to the amplitude $A = A_0 = 1265$ Pa. The error bars in ϕ are obtained using the maximum and minimum estimated values of the profile height h that, as discussed in the text, is harder to evaluate in optical mismatch conditions. Inset: Dependence of the amplitude A on depletant concentration, fitted with a straight line (symbols are the same as in the figure body).

4. Discussion

Our measurements suggests the following simple description of the compressive properties of depletion gels. Upon spinodal decomposition, clusters at a volume fraction ϕ_c, which barely depends on the strength of the attractive interaction, form. Under the effect of the centrifugal forces, these gels progressively compact, showing a compressive yield stress $\Pi(\phi)$ that grows as a power-law of ϕ, until the average volume fraction approximately reaches ϕ_c. For larger values of ϕ, the compressive yield stress dramatically rises, showing that is much harder to compress gels whose average fraction exceed ϕ_c. Nevertheless, the gels still display a finite compressibility,

until their volume fraction reaches a value comparable to the r.c.p. for hard spheres. It is then very tempting to associate ϕ_c with the volume fraction of the liquid branch of the coexistence line. In this view, the rather abrupt change of the compressive yield stress provides an estimate of the value of ϕ_c, obtained by macroscopic rheological methods. The evidence we collected, therefore, seems to support the suggestion made in [5] that the value of ϕ_c basically coincides with the liquid branch of the coexistence curve.

Conversely, both the values we found for ϕ_c and their basic independence of the interaction strength do not seem to agree with the results given in [11]. Recall however that the interpretation of the latter was crucially based on the fact that, at variance with what we found, the dense phase turns out to be basically incompressible. It is then worth wondering why the depletion gels we investigate and the protein gel studied in [12] display such a different compressive behaviour. A possible explanation is the following. From figure 4 we notice that, for the gels we investigated, the minimal relative centrifugal force value $\mathrm{RCF}_{\mathrm{min}}$ required to enter the second, diverging yield stress regime is about $100g$. At the same time, for a wide class of colloidal gels, the yield stress is found to scale as the inverse of the square of the particle size [19, 20]. Let us then make a rough evaluation of the corresponding value $\mathrm{RCF}'_{\mathrm{min}}$ for lysozyme, assuming that this scaling holds in general, and that the strength of the attractive interparticle forces holding together depletion and protein gels are comparable. In terms of the MFA and lysozyme particle radii, a and a', and of the density differences with the solvent, $\Delta\rho$ and $\Delta\rho'$, this yields

$$\mathrm{RCF}'_{\mathrm{min}} = \frac{\Delta\rho}{\Delta\rho'}\left(\frac{a}{a'}\right)^2 \mathrm{RCF}_{\mathrm{min}}.$$

Taking $a = 90\,\mathrm{nm}$, $a' = 2.5$ nm, $\Delta\rho = 1.14$ g ml^{-1}, and $\Delta\rho' = 0.35$ g ml^{-1}, one finds $\mathrm{RCF}'_{\mathrm{min}} \simeq 4 \times 10^5$, which is more than one order of magnitude larger than the maximal centrifugal acceleration used in the experiments reported in [12]. This simple calculation suggests that the final compression regime is extremely hard to be accessed for protein gels, because of their much larger compressive yield stress.

Acknowledgments

We thank Emanuela Zaccarelli, Patrick Charbonneau and Luca Cipelletti for insightful discussions.

ORCID iDs

Enrico Lattuada https://orcid.org/0000-0002-8537-0988
Stefano Buzzaccaro https://orcid.org/0000-0002-7394-5262
Roberto Piazza https://orcid.org/0000-0001-7398-0335

References

[1] Miller M A and Frenkel D 2004 Phase diagram of the adhesive hard sphere fluid *J. Chem. Phys.* **121** 535–45
[2] Buzzaccaro S, Rusconi R and Piazza R 2007 'Sticky' hard spheres: equation of state, phase diagram, and metastable gels *Phys. Rev. Lett.* **99** 098301
[3] Zaccarelli E 2007 Colloidal gels: equilibrium and non-equilibrium routes *J. Phys.: Condens. Matter* **19** 323101
[4] Manley S *et al* 2005 Glasslike arrest in spinodal decomposition as a route to colloidal gelation *Phys. Rev. Lett.* **95** 238302
[5] Lu P J, Zaccarelli E, Ciulla F, Schofield A B, Sciortino F and Weitz D A 2008 Gelation of particles with short-range attraction *Nature* **453** 499
[6] Brambilla G, Buzzaccaro S, Piazza R, Berthier L and Cipelletti L 2011 Highly nonlinear dynamics in a slowly sedimenting colloidal gel *Phys. Rev. Lett.* **106** 118302
[7] Buzzaccaro S, Secchi E, Brambilla G, Piazza R and Cipelletti L 2012 Equilibrium concentration profiles and sedimentation kinetics of colloidal gels under gravitational stress *J. Phys.: Condens. Matter* **24** 284103
[8] Secchi E, Buzzaccaro S and Piazza R 2014 Time-evolution scenarios for short-range depletion gels subjected to the gravitational stress *Soft Matter* **10** 5296–310
[9] Bartlet P, Teece L J and Faers M A 2012 Sudden collapse of a colloidal gel *Phys. Rev.* E **85** 021404
[10] Zia R N, Benjamin J and Russel W B 2014 A micro-mechanical study of coarsening and rheology of colloidal gels: cage building, cage hopping, and Smoluchowski's ratchet *J. Rheol.* **58** 1121
[11] Gibaud T and Schurtenberger P 2009 A closer look at arrested spinodal decomposition in protein solutions *J. Phys.: Condens. Matter* **21** 322201
[12] Cardinaux F, Gibaud T, Stradner A and Schurtenberger P 2007 Interplay between spinodal decomposition and glass formation in proteins exhibiting short-range attractions *Phys. Rev. Lett.* **99** 118301
[13] Piazza R 2014 Settled and unsettled issues in particle settling *Rep. Prog. Phys.* **77** 056602
[14] Degiorgio V, Piazza R, Bellini T and Visca M 1994 Static and dynamic light scattering study of fluorinated polymer colloids with a crystalline internal structure *Adv. Colloid Interface Sci.* **48** 61–91
[15] Dzuy N Q and Boger D V 1985 Direct yield stress measurement with the vane method *J. Rheol.* **29** 335–47
[16] Liddell P V and Boger D V 1996 Yield stress measurements with the vane *J. Non-Newton. Fluid Mech.* **63** 235–61
[17] de Kretser R G, Boger D V and Scales P J 2003 Compressive rheology: an overview *Rheol. Rev.* 125–65
[18] Buscall R and White L R 1987 The consolidation of concentrated suspensions. Part 1—the theory of sedimentation *J. Chem. Soc. Faraday Trans.* **83** 873–91
[19] Kim C *et al* 2007 Gravitational stability of suspensions of attractive colloidal particles *Phys. Rev. Lett.* **99** 028303
[20] Zhou Z, Solomon M J, Scales P J and Boger D V 1999 The yield stress of concentrated flocculated suspensions of size distributed particles *J. Rheol.* **43** 651–71